The Bronnikov Aided Correction for X-ray Computed Tomography

Y. De Witte, M. Boone, J. Vlassenbroeck, M. Dierick and L. Van Hoorebeke

Dept. of Subatomic and Radiation Physics, Proeftuinstraat 86, 9000 Ghent, Belgium

Yoni.DeWitte@UGent.be

This paper was published in *Journal of the Optical Society of America A* and is made available as an electronic reprint with the permission of OSA. The paper can be found at the following URL on the OSA website: http://dx.doi.org/10.1364/JOSAA.26.000890. Systematic or multiple reproduction or distribution to multiple locations via electronic or other means is prohibited and is subject to penalties under law.

Abstract: When a very low absorbing sample is scanned at an X-ray CT-setup with a microfocus X-ray tube and a high resolution detector, the obtained projection images not only contain absorption contrast, but also phase contrast. While images without a phase signal can be reconstructed very well, such mixed phase and absorption images give rise to severe artefacts in the reconstructed slices. In this paper, a method is described that applies a correction to these mixed projections, in order to remove the phase signal. These corrected images can then be processed using a standard filtered back projection algorithm to obtain reconstructions with only little or no phase artefacts. This new method, which we call the Bronnikov Aided Correction (BAC), can be used in a broad variety of applications and without much additional effort. It is tested on a biological and a pharmaceutical sample, results are evaluated and discussed by comparing them with conventional reconstruction methods.

OCIS codes: 100.5070, 110.3010, 110.6955, 110.7440.

References and links

1. X. Wu, "X-ray cone-beam phase tomography formulas based on phase-attenuation duality," Optics Express **13**(16), 6000–6014 (2005).
2. R. A. Lewis, "Medical phase contrast x-ray imaging:current status and future prospects," Physics in Medicine and Biology **49**(16), 3573–3583 (2004).
3. A. C. Kak and M. Slaney, *Principles of Computerized Tomographic Imaging* (IEEE Press, 1988).
4. F. Natterer, *The Mathematics of Computerized Tomography* (SIAM, Philadelphia, 2001).
5. C. Kottler, F. Pfeiffer, O. Bunk, C. Grünzweig, and C. David, "Grating interferometer based scanning setup for hard x-ray phase contrast imaging," Review of Scientific Instruments **78**, 043,710 (2007).
6. A. Bronnikov, "Reconstruction formulas in phase-contrast tomography," Optics Communications **171**, 239–244 (1999).
7. M. Engelhardt, J. Baumann, M. Schuster, C. Kottler, F. Pfeiffer, O. Bunk, and C. David, "High-resolution differential phase contrast imaging using a magnifying projection geometry with a microfocus x-ray source," Applied Physics Letters **90**(22), 224,101 (2007).

8. S. C. Mayo, T. J. Davis, T. Gureyev, P. R. Miller, D. Paganin, A. Pogany, A. Stevenson, and S. Wilkins, "X-ray phase-contrast microscopy and microtomography," Optics Express **11**(19), 2289–2302 (2003).
9. T. E. Gureyev, "Composite techniques for phase retrieval in the Fresnel region," Optics Communications **220**, 49–58 (2003).
10. M. A. Anastasio, D. Shi, F. De Carlo, and X. Pan, "Analytic image reconstruction in local phase-contrast tomography," Physics in Medicine and Biology **49**, 121–144 (2004).
11. M. R. Teague, "Image formation in terms of the transport equation," J. Opt. Soc. Am. A **2**(11), 2019–2027 (1985).
12. A. Bronnikov, "Theory of quantitative phase-contrast computed tomography," Journal of the Optical Society of America A **19**(3), 472–480 (2002).
13. A. Groso, R. Abela, and M. Stampanoni, "Implementation of a fast method for high resolution phase contrast tomography," Optics Express **14**(18), 8103–8110 (2006).
14. B. Masschaele, V. Cnudde, M. Dierick, P. Jacobs, L. Van Hoorebeke, and J. Vlassenbroeck, "UGCT: New x-ray radiography and tomography facility," Nuclear Instruments and Methods in Physics Research A **580**(1), 266–269 (2007).
15. J. Vlassenbroeck, M. Dierick, B. Masschaele, V. Cnudde, L. Van Hoorebeke, and P. Jacobs, "Software tools for quantification of X-ray microtomography," Nuclear Instruments and Methods in Physics Research A **580**(1), 442–445 (2007).

1. Introduction

In X-ray Computed Tomography (CT), a sample is investigated by taken a series of X-ray transmission images under different angles. These projection images contain information about the X-ray absorption coefficients of the different materials in the sample and are used to obtain a 3D representation of the sample. However, when looking at a very low absorbing sample, the projection images are distorted because the X-rays passing through the sample experience a phase shift. A technique which utilizes these shifts is known as phase-contrast CT, and it can be used to detect very small features that are not visible with absorption CT [1, 2]. In theory, one can use either a purely absorption image, or a pure phase image to reconstruct the sample. However, when reconstructing such mixed phase and absorption projections with the standard filtered back projection algorithm [3, 4], the phase-shift signal gives rise to severe artefacts, which results in bad reconstructions, containing negative densities and wrongfully emphasized edges. These phase shifts and their resulting artefacts impose a limit on the resolution that can be achieved at a conventional X-ray CT setup using an X-ray tube. A solution to this problem exists by using gratings [5], but these are expensive and complicate the experimental setup. A. Bronnikov suggested another solution [6] which consists of applying a filter to the projection images that converts the phase signal so that it can be reconstructed using the standard filtered back projection algorithm. Others have followed similar approaches, which are all based on phase retrieval methods [7, 8, 9, 10]. In contrast with these methods however, the authors present in this paper a technique that corrects for the phase signal, so the absorption signal can be reconstructed without artefacts. The proposed method, named Bronnikov Aided Correction (BAC), uses the Bronnikov-filter to identify the phase signal, and then uses this signal to correct the original projection images. These corrected images can then be reconstructed using the standard filtered back projection algorithm, without suffering from heavily disturbing phase artefacts. This alternative approach can be used at any conventional X-ray CT setup that uses an X-ray tube and it does not require an additional scan or some a priori knowledge about the sample. Therefore, it can be easily applied in a broad range of applications without much additional effort.

2. Theoretical background

2.1. Bronnikov filter

The filter presented by Bronnikov is based on the Transport of Intensity Equation (TIE) [11]. The intensity distribution $I_{\theta,z}(x,y)$ at a distance z from the sample and angle of rotation θ can,

for weakly absorbing samples and distances d in the near Fresnel region, be expressed as [12]:

$$I_{\theta,d}(x,y) = I_{\theta,0}(x,y)\left[1 - \frac{\lambda d}{2\pi}\nabla^2\phi_\theta(x,y)\right], \tag{1}$$

where $I_{\theta,0}(x,y)$ is the absorption-contrast intensity measured at $z=0$, λ is the X-ray wavelength and $\phi_\theta(x,y)$ is the phase function of the object.

Based on this equation, Bronnikov derived a filter that needs to be applied to the original projection data. This filter however is only applicable when the distribution $I_{\theta,0}(x,y)$ is known, which can be found by scanning the sample in the contact print plane. Groso et al. [13] added a correction factor to the filter, which allows the filter to be used without knowledge of $I_{\theta,0}(x,y)$ and thus without requiring an extra scan. The two-dimensional Fourier transform of this filter has the following form [13]:

$$q(\xi,\eta) = \frac{|\xi|}{\xi^2+\eta^2+\alpha}, \tag{2}$$

where ξ and η are the spatial frequencies and α is an absorption dependent correction parameter. This parameter α is found in a semi-empirical way by evaluating some filtered projections.

For a practical implementation, this filter can be separated into two parts:

$$q(\xi,\eta) = p(\xi,\eta)r(\xi), \tag{3}$$

where $r(\xi)$ is the regular ramp filter:

$$|\xi|, \tag{4}$$

which is already part of the standard filtered back projection algorithm. The phase filter $p(\xi,\eta)$, given by:

$$p(\xi,\eta) = \frac{1}{\xi^2+\eta^2+\alpha}, \tag{5}$$

is a 2D-filter that needs to be applied to the projection images.

When applying the phase filter (5) to the original projection images, the absorption signal is eliminated and the phase signal is converted to a set of line integrals $\phi_\theta(x,y)$ which contains information about the phase coefficients φ of the sample:

$$\phi_\theta(x,y) = \int \varphi dL, \tag{6}$$

where the integral is taken along the path of the ray starting at the source and ending in the detector pixel with coordinates (x,y).

In conventional absorption CT, a projection consists of a set of line integral $I_\theta(x,y)$ containing information about the attenuation coefficients μ of the sample, given by:

$$-\ln(I_\theta(x,y)) = \int \mu dL. \tag{7}$$

From the above and from (3) it follows that the projection data can be reconstructed by first applying the phase filter (5) to the original projection data, and then reconstructing the filtered data by using the standard filtered back projection algorithm. This method will further be referred to as the Modified Bronnikov Algorithm (MBA).

2.2. BAC method

The Bronnikov Aided Correction (BAC) that is presented in this paper is based on the Bronnikov approach described in the previous section. However, instead of using the phase signal to reconstruct the phase coefficients φ of the object, this information is used to correct the original projection images and obtain a pure absorption image, from which the attenuation coefficients μ of the object can be reconstructed. According to (1), it is possible to obtain the pure absorption image $I_{\theta,0}(x,y)$ from the mixed projection $I_{\theta,d}(x,y)$ when the function $\phi_\theta(x,y)$ is known:

$$I_{\theta,0}(x,y) = \frac{I_{\theta,d}(x,y)}{1 - \frac{\lambda d}{2\pi}\nabla^2\phi_\theta(x,y)}. \tag{8}$$

For the proposed BAC algorithm, the original projection images are first filtered using the Bronnikov filter, resulting in the phase function $\phi_\theta(x,y)$. Then the correction function $C_\theta(x,y)$ is calculated:

$$C_\theta(x,y) = 1 - \gamma \cdot \nabla^2\phi_\theta(x,y), \tag{9}$$

where we replaced the coefficient $\lambda d/(2\pi)$ by the parameter γ which allows us to control the amplitude of the correction. The value of this parameter can be chosen with only little effort, by evaluating line profiles of a single, corrected image. Finally, we divide the original projections $I_{\theta,d}(x,y)$ by the correction function $C_\theta(x,y)$ and obtain the corrected projection $I_{\theta,0}(x,y)$, which should now only contain the absorption signal. This set of corrected projections can then be reconstructed using the standard filtered back projection algorithm. This will be referred to as the BAC method.

3. Results and discussion

The BAC algorithm is tested on a biological and a pharmaceutical sample. Results are compared with reconstructions obtained by regular filtered back projection (FBP) and by the Modified Bronnikov Algorithm (MBA). The scans of the samples were taken at the Centre for X-ray Tomography (UGCT) of the Ghent University, Belgium [14]. The X-ray tube is a Feinfocus FXE-160.51, with a focal spot size of 900 μm, the tube is operated at 60 kV. The detector used is a Photonic Science VHR, which has 2667 x 4008 pixels and a 6 μm thick Gadox screen as scintillator. The pixels are rebinned by a factor of 4, giving an effective pixel size of 38 μm. The standard filtered back projection is performed by using the tomographic reconstruction package Octopus [15]. 3D renderings of the reconstructed objects are made using VGStudioMax 2.1 (Volume Graphics).

3.1. Biological sample: leg of a fly

The first sample to illustrate the effect of the BAC algorithm is the leg of a fly. The diameter of the leg is approximately 100 μm. In figure 1, line profiles of the original projection and the BAC image are compared for different values of the parameter γ. The profile shows the transition between the edge of the leg and the surrounding air. If the parameter is too low (γ_1, γ_2 and γ_3), the phase signal becomes smaller but it does not completely vanish. If the parameter is too high (γ_5 and γ_6), the phase signal simply gets inverted. A good choice of the parameter (γ_4) can (almost) entirely correct for the phase signal and remove it from the line profile. Looking at the projection images in figure 2, one can see that the bright and dark bands in the original image (left image) have almost completely disappeared in the BAC image (right image), while the level of detail of the internal structure of the leg has been preserved. To see the effect of the phase correction, one should concentrate for instance on the white borderline on the left edge of the leg in the original projection, indicated by the arrow. This bright border is a typical phase effect that can be observed in this kind of samples. Comparing this region with the BAC image,

one can notice how this border has been corrected for. The middle image shows the original projection after the Bronnikov phase filter has been applied, it does not contain any phase. Based on such line profiles and single projections, the parameter γ in (9) can be selected.

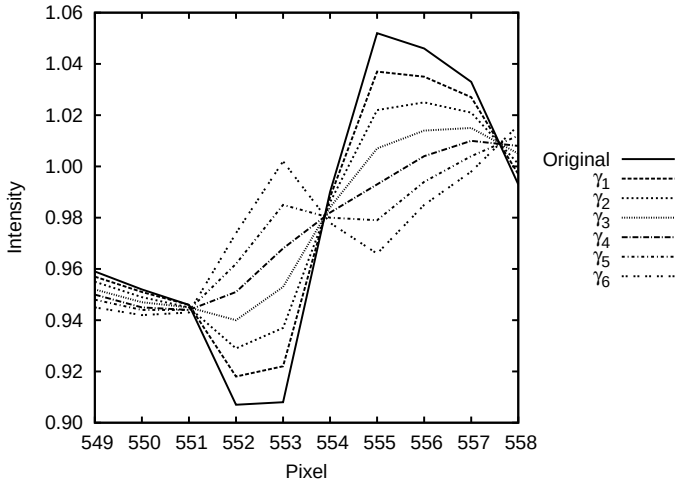

Fig. 1. Line profiles of the transition between the edge of the leg and the surrounding air, for the original projection and for the BAC projection with different values of the parameter γ.

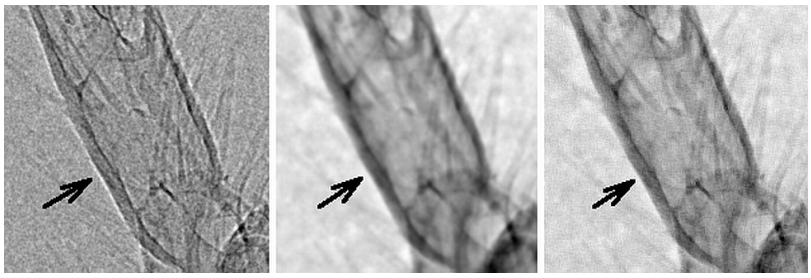

Fig. 2. Left: original projection image of the leg. Middle: projection image after applying the Bronnikov phase filter. Right: projection image after BAC.

Now, the full set of projections can be corrected and the volume can be reconstructed using a standard filtered back projection algorithm. Three different reconstructions of the leg were performed, according to the method used, they will further be referred to as the FBP, MBA and BAC reconstruction, for the reconstruction of, respectively, the original projections, the projections filtered with the Modified Bronnikov phase filter and the projections corrected by the BAC method.

The central slice of the reconstructions is shown in figure 3. The minimum gray value for these slices is clipped at 0, so that only positive values of the reconstructed coefficients are displayed. As one can see, the three slices are clearly different from each other. The FBP slice (left image) is very sharp, but the reconstruction suffers from severe phase artefacts. Due to these artefacts, structures that should be rather homogeneous appear to consist of a very dense edge and an inner region with a very low density, which is in fact hardly distinguishable from the background noise. When looking at the MBA (middle image) and the BAC (right image)

slices, these structures look much more realistic. In the MBA slice, the phase artefacts have almost completely disappeared, but the slice has become more blurry, thus losing some detail. The BAC slice, on the other hand does not suffer from this blurring and remains very sharp, while the phase artefacts have been heavily reduced. Also note that both MBA and BAC result in lower relative noise levels compared to FBP.

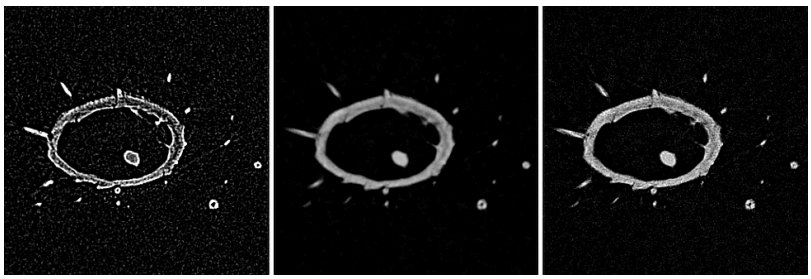

Fig. 3. A slice of the reconstructed leg of a fly. Left: FBP, middle: MBA, right: BAC.

To further investigate the differences between the three methods, and to show the advantage of the BAC method, figures 4 and 5 show 3D renderings of the reconstructions. In figure 4, a horizontal cut is made through the 3D model of the leg, revealing its internal structure. As one can see, the artefacts in the FBP reconstruction wrongfully suggest that the structures of the leg seem to consist of hollow region between dense surfaces. For both the MBA and BAC reconstructions, these structures are filled. In contrast with the MBA reconstruction, the BAC reconstruction still reveals details in the structures of the leg. This difference can be clearly seen when one looks at the left side of the images. The BAC image reveals gaps in the outer structures of the leg, which cannot be detected in the MBA image. A second 3D rendering (figure 5) shows a detail of the outer structure of the leg. From the FBP and BAC images, it is seen that the leg is covered by a bubble-like texture, which is severely blurred in the MBA image.

Fig. 4. Horizontal cut through the 3D rendered model of the reconstructed leg. Left: FBP, middle: MBA, right: BAC.

From these three comparative figures, it can easily be concluded that the FBP reconstruction fails because of the strong presence of phase artefacts. The MBA and BAC method reconstruct mixed projections very well, but the MBA method seems to suffer from a blurring effect, thereby losing some detail. The BAC method keeps these details intact, resulting in a sharper reconstruction. One must hereby note however that, although both methods produce similar images, they actually reconstruct different values: the MBA method reconstructs the phase coefficients φ, while BAC reconstructs the attenuation coefficients μ.

Considering the experimental setup, it is not surprising that the MBA method results in rather blurry images. Due to the polychromacy of the X-rays, the phase shifts in the original projections are not sharply outlined. Instead, they are smeared over several pixels (see figure 1). While

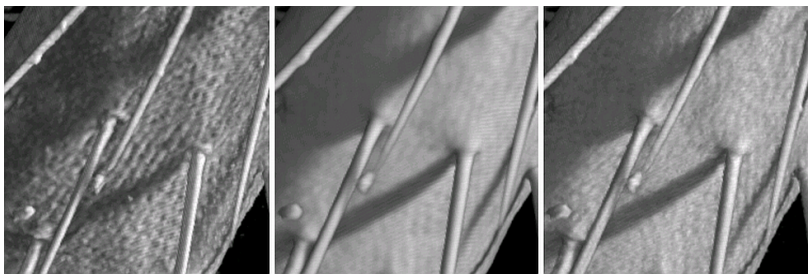

Fig. 5. Detail of the 3D rendered model of the reconstructed leg. Left: FBP, middle: MBA, right: BAC.

the BAC method removes this signal, the MBA uses only this smeared signal for the reconstruction, thus resulting in slightly blurred images.

3.2. Pharmaceutical sample: bead

The second sample under study is a bead. The diameter of the bead is about 850 μm. It consists of a dense core surrounded by a less dense mantle. Both core and mantle consist of homogeneous material and contain air inclusions. The structure of the core and mantle are important in pharmaceutical product development, since they determine the solubility of the bead.

Figure 6 shows a cross-section of the bead, reconstructed with the FBP, MBA and BAC method. On all three images, one can easily distinct mantle and core. However, in the FBP slice, two more components can be detected. The first is a dense border that surrounds the beads mantle. Second, there is a faint black and white borderline running between the mantle and the core. Both components do not represent any physical feature, but are easily identified as phase artefacts. Other phase artefacts can be observed in the form of a thin, white border surrounding the different air inclusions. In the MBA slice, these artefacts have been completely removed, but the slice is severely blurred when compared to the FBP and BAC slices. Also, in the MBA slice, the mantle (and also the core, but in a more subtle way) is not homogeneous, but seems to become more dense when moving away from the beads centre. This cupping is thought to be due to the relative high absorption of the sample (only about 75% transmission through the centre of the bead), in which case the Modified Bronnikov filter (2) may no longer be adequate. In the BAC slice, the phase artefacts around the mantle and between the mantle and core have vanished. Phase artefacts surrounding the inclusions have been heavily reduced. Both mantle and core show no signs of cupping and are very homogeneous, while all details are preserved.

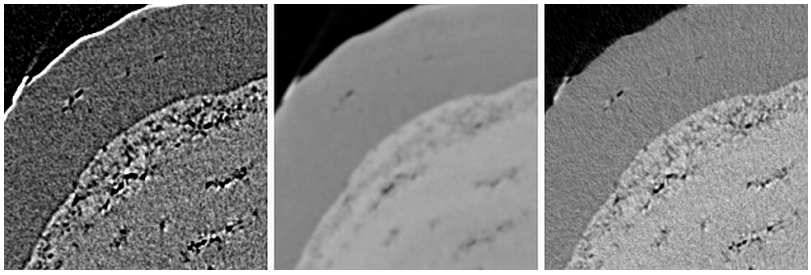

Fig. 6. Reconstructed slice of the bead. Left: FBP, middle: MBA, right: BAC.

A last set of images (figure 7) shows a 3D rendering of a cut through the outer edge of the

mantle. Again, it can be seen that the FBP reconstruction suggests a dense border surrounding the surface. Such a border can also be seen in the MBA image, but here, it is due to the cupping instead of phase artefacts. This wrongfully emphasized border is not present in the BAC reconstruction, which instead shows a highly homogeneous mantle with a very clean transition between the mantle and the air around the bead. The BAC image also reveals much more detail on the mantles surface than the MBA image.

This sample again shows that the BAC method can deal with phase artefacts very well, without reducing the sharpness and level of detail of the reconstructions.

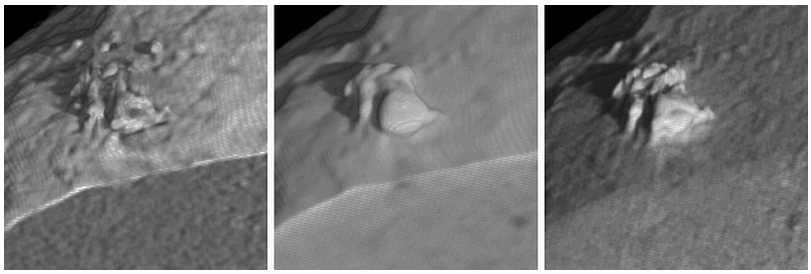

Fig. 7. Detail of a cut through the 3D rendered model of the bead. Left: FBP, middle: Bronnikov, right: BAC.

4. Conclusion

In this paper, a method is presented to correct phase artefacts at an X-ray CT setup containing a microfocus X-ray tube. The proposed method, named Bronnikov Aided Correction (BAC), is tested on a biological and a pharmaceutical sample and results are compared with a conventional filtered back projection algorithm and the Bronnikov phase filter. The reconstructions of the corrected projections contain almost no phase artefacts, while the detail detectability is maintained. The BAC method is thus shown to be an excellent technique for reconstructing mixed phase and absorption projections. Since the method requires no additional hardware, projection data or a priori information, it can be easily used at any X-ray CT setup. Therefore, the benefits and the potential applications of the BAC method have been clearly illustrated.